Particle Diffusion in a Quasi-Two-Dimensional Bacterial Bath

Xiao-Lun Wu[1,2] and Albert Libchaber[1,3]

[1]*NEC Institute, 4 Independence Way, Princeton, New Jersey 08540*

[2]*Department of Physics, University of Pittsburgh, Pittsburgh, Pennsylvania 15260*

[3]*Center for Studies in Physics and Biology, Rockefeller University, New York, New York 10021*

(Received 27 April 1999)

We study the effect of bacterial motion on micron-scale beads in a freely suspended soap film. Given the sizes of bacteria and beads, the geometry of the experiment is quasi-two-dimensional. Large positional fluctuations are observed for beads as large as 10 μm in diameter, and the measured mean-square displacements indicate superdiffusion in short times and normal diffusion in long times. Though the phenomenon is similar to Brownian motions of small particles, its physical origin is different and can be attributed to the collective dynamics of bacteria.

PACS numbers: 87.17.Jj, 45.70.Qj, 87.18.Hf

The incessant motion of particles in a fluid is due to multiple collisions of the particles with the surrounding fluid molecules. In this classical picture of Brownian motion both the particles and fluid molecules are passive, driven by thermal fluctuations. In this paper we study a new situation with two types of particles in a fluid, but one of them is active and the other passive. Explicitly, we study the motion of micron-scale beads in a bath of bacteria. The problem is biologically relevant in that motility of microorganisms not only reflects their survival strategies, resulting from millions of years of evolution, but also helps maintain the ecological balance by active transport of nutrients in aqueous environments. A concentrated population of swimming bacteria is also a nonlinear dynamical system, exhibiting spatiotemporal patterns that are of interest to physical scientists [1].

A particular feature of our experiment is that the geometry is quasi-two-dimensional; the beads and bacteria coexist in a freely suspended horizontal soap film. The use of such a film significantly reduces hydrodynamic dissipation to its surroundings, as the shear viscosity of air is only $1/100$ of the film. One observes that large beads fluctuate wildly with the mean-square displacement (MSD) displaying two regimes in time. For short times ($t < t_C$), the MSD is superdiffusive, whereas for long times ($t > t_C$), normal diffusion is recovered. Though the effect appears to be similar to the underdamped to overdamped transition in Brownian systems, the crossover in our experiment is not due to the particles' inertia. Rather it is a result of transient formations of coherent structures, swirls and jets, in the bacterial bath. The t_C is thus the lifetime of these coherent structures and is found to increase linearly with the bacterial density n. If an effective temperature T_{eff} would be assigned to the motion of the beads, it follows from the Stokes-Einstein relation that T_{eff} is $2-3$ orders of magnitude larger than room temperature [2].

The bacteria used were a wildtype *Escherichia coli* (RP437), which have been studied extensively for their chemotactic behavior [3–5]. The cell body is typically 1 μm in diameter and $2-3$ μm in length. The bacteria swim by rotating several flagella at a frequency of about 100 Hz. To facilitate video imaging and tracking, the bacteria were transformed to carry a plasmid which expressed green fluorescence proteins (GFP) [6]. The bacteria were grown using a standard protocol, washed, and resuspended in a motility medium [5]. The stock solution contained $n \simeq 5.4 \times 10^{10}$ cells/cm^{-3}, corresponding to 10% in volume. Other concentrations were obtained by dilution with the motility solution along with a trace amount of polystyrene (PS) spheres.

In order to draw a stable film, surfactant IGEPAL (Sigma) was added to each sample. This is a nonionic surfactant with a critical micellar concentration (cmc) $\phi_c = 0.83$ mM. Test runs with $0.01 < \phi < 100$ cmc indicated that IGEPAL had no discernible effect on bacterial swimming either in the bulk or in the film. In the measurements therefore $\phi = \phi_c$ was kept constant for all samples. A soap film (0.4×0.4 cm^2) seeded with PS particles was supported on four thin glass fibers and maintained in a humidity chamber. Figure 1 is a schematic of the chamber along with a fluorescence image of the film containing 10 μm PS beads and the bacteria. The finite exposure time (0.03 s) caused the tracks of the bacteria to be somewhat smeared but not those of the beads. The film thickness was approximately the diameter of the beads, as confirmed by focusing the microscope at different depths in the film.

Phase contrast microscopy was used to follow the motion of the PS beads. The images were digitized and analyzed using a PC. To better characterize the motion of the beads, the velocity distribution of the bacteria was also measured. The GFPs incorporated in *E. coli* cells made their visualization simple by fluorescence microscopy. A series of images, $1/30$ s apart, allowed swimming velocity of individual bacteria to be measured and the velocity distribution $P(v)$ calculated. Experimentally $P(v)$ was found to obey the Maxwell's distribution, $P(v) = \frac{2|v|}{v_0^2} \exp(-\frac{v^2}{v_0^2})$, with $v_0 \simeq 20$ μm/s.

Visual observation showed that for small densities bacteria tended to swim more smoothly in the film than in the

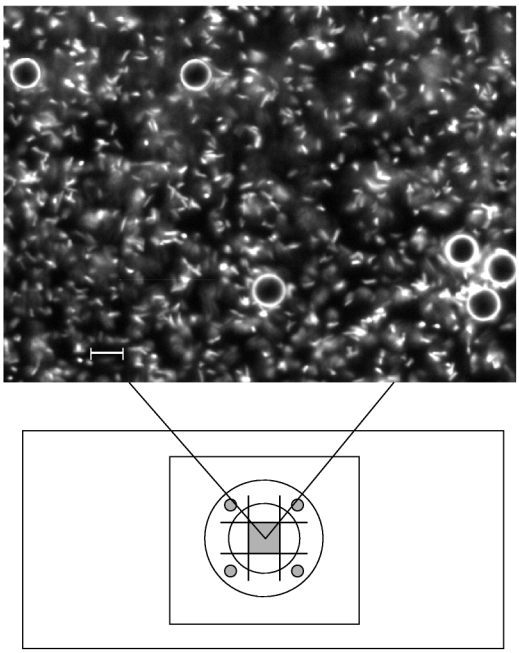

FIG. 1. The experimental setup and the fluorescence image of *E. coli* with 10 μm PS spheres. The soap film, the square gray area in the figure, was enclosed in an aluminum cell with glass windows. The humidity in the cell was maintained by four water drops as indicated. The scale bar is 10 μm.

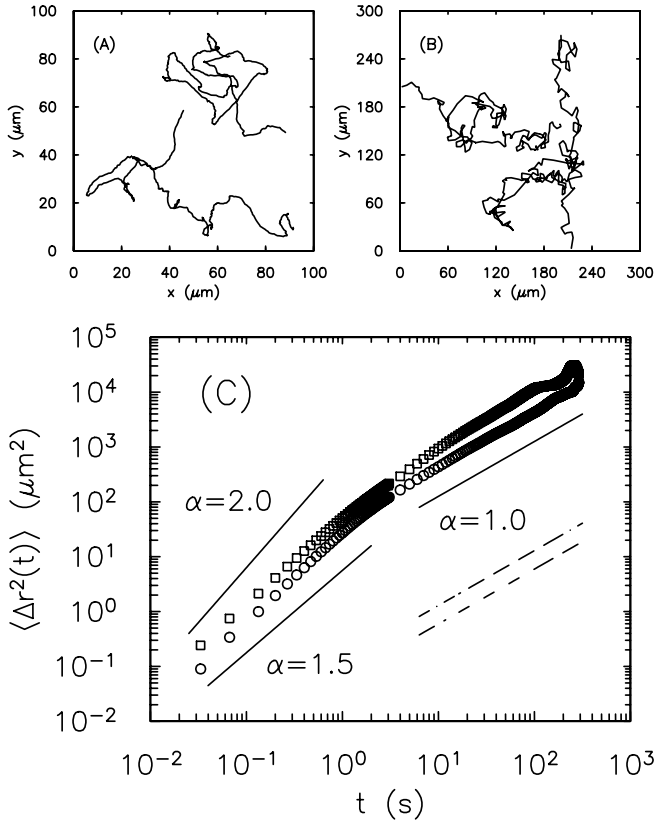

FIG. 2. (A) Motion of two 10 μm beads followed for 20 s. (B) The same beads followed for 3 min. (C) The MSD measurements of PS beads with diameters 4.5 (squares) and 10 μm (circles) are shown. The bead concentrations were $\sim 10^{-3}$ μm^{-2}. The solid lines with slopes $\alpha = 2.0$, 1.5, and 1.0 are guides to the eyes. The two dashed lines correspond to the thermal diffusion of 4.5 and 10 μm particles, respectively.

bulk fluid; i.e., they did not tumble as frequently. This was partly due to the restricted space of the film and partly to the nutritional condition of the medium. In high densities, however, collisions between bacteria and hydrodynamic dispersion randomized their swimming directions, yielding a velocity distribution that was identical to that of an ideal gas. A striking observation was that the positions of the beads, as large as 10 μm in diameter, fluctuated strongly as delineated in Figs. 2(A) and 2(B). This is in sharp contrast with Brownian motion of these particles that showed no discernible motion in the absence of bacteria. Particle tracks, such as those in Fig. 2, allowed the MSD to be calculated: $\langle \Delta r^2(t) \rangle = \frac{1}{N} \sum_i \langle [\vec{r}_i(\tau + t) - \vec{r}_i(\tau)]^2 \rangle_\tau$. Here both the time and the particle averages were used, with N and i being the number and the index of individual beads. In typical measurements ten to a hundred particle tracks were followed up to 5 min.

Figure 2(C) shows a set of measurements with two different beads of diameters $2R = 4.5$ and 10 μm, but with the same bacterial concentration $n \sim 10^{10}$ cm^{-3}. As can be seen, the data were extensive, spanning several decades in time. The two measurements gave nearly identical trends, despite different particles used. For short times ($0.03 < t < 1$ s), diffusion appeared to be anomalous with $\langle \Delta \vec{r}^2(t) \rangle \propto t^\alpha$, where $1.5 < \alpha < 2.0$. For long times ($10 < \tau < 300$ s), however, the data were consistent with normal diffusion, with $\alpha \simeq 1.0$. The above measurements suggested that there was certain persistence in the particle motion induced by bacterial bombardments in short times. This was consistent with the visual observation [see Fig. 2(A)] which showed that particle tracks consisted of straight segments of different lengths, indicative of ballisticlike motion. For sufficient long times [see Fig. 2(B)], particle tracks were randomized, giving rise to Brownian-like behavior.

Heuristically, one can define an effective long-time diffusion coefficient $D_{\text{eff}} = \frac{1}{4} \delta \langle \Delta r^2(\tau) \rangle / \delta t$, where the finite time difference δt is taken to be the longest time of the measurements, $200 < t < 300$ s. In this case one finds $D_{\text{eff}} \simeq 1.0 \times 10^{-6}$ cm^2/s and 4.3×10^{-7} cm^2/s for the 4.5 and 10 μm beads, respectively. This observation allows us to draw a few interesting conclusions: (i) It suggests that $D_{\text{eff}} \propto 1/R$, which has the same R dependence as the Stokes-Einstein relation, $D_T = k_B T / 6\pi\eta R$, where $\eta \sim 0.01$ poise is the viscosity of the fluid. Such a result is expected for a system at thermal equilibrium, but not for a nonequilibrium system such as ours. (ii) Since in a previous experiment it was shown that the thermal diffusion coefficient for the beads in the film is of the same order of magnitude as that in the corresponding bulk fluid [7], it follows from the Stokes-Einstein relation that

$D_T \sim 10^{-9}$ cm^2/s for both particles. This implies that the effective temperature of the bacterial bath is about 100 times greater than room temperature.

We next turned our attention to the effects of bacterial concentration n on the motion of 10 μm beads. It was observed that as n increases the particle motion became more energetic. Inspection of background motion of bacteria with a large n revealed intermittent large-scale flows in the form of swirls and occasionally jets. The typical scale of the swirls was roughly 10–20 μm. Figure 3 shows a set of measurements with $n = 0.67$, 1.34, and 5.35×10^{10} cm^{-3}. On this log-log plot the MSD data are again rather similar for different n, consisting of two different regimes as in Fig. 2(C). The most noticeable feature of the plot is a remarkable increase of the characteristic time t_C (see vertical arrows), which marks the crossover from the short- to the long-time regimes as n increases. Correspondingly, there is a length scale $\ell_C (\equiv \sqrt{\langle \Delta r^2(t_C) \rangle})$ which also increases with n. For the highest concentration, $t_C \simeq 2$ s and $\ell_C \simeq 10$ μm. The latter is comparable to the swirl size observed visually.

A simple calculation shows that even for 10 μm beads the short-time persistent motion cannot be due to the particles' inertia. This is because their motion is strongly damped in the viscous fluid with a typical damping time $t_0 = m/\gamma \simeq 10^{-5}$ s, too short to be seen in the measurement. Here m is the particle mass and $\gamma = 6\pi\eta R$ is the frictional coefficient. Our observations therefore suggest that forces on the beads are not random but correlated over certain spatial and temporal scales. Such correlations must be related to the spontaneous formation of swirls in the bacterial bath. To model dynamic fluctuations of the beads, we wrote a simple Langevin-type equation with the "collisional force" that is exponentially correlated in time:

$$m \frac{d\vec{v}}{dt} = -\gamma \vec{v} + \vec{f}(t), \tag{1}$$

$$\langle \vec{f}(t) \rangle = 0, \tag{2}$$

$$\langle \vec{f}(0) \cdot \vec{f}(t) \rangle = \frac{4D\gamma^2}{t_C} \exp(-t/t_C), \tag{3}$$

where D is an effective diffusion coefficient of a test particle immersed in the bacterial bath, and t_C is the lifetime of the swirls. From Eqs. (1)–(3), the particle velocity autocorrelation function could be derived in the limit $t_C \gg t_0$,

$$\langle \vec{v}(t) \cdot \vec{v}(0) \rangle = \langle v(0)^2 \rangle \exp(-t/t_C), \tag{4}$$

where $\langle v(0)^2 \rangle = 2D/t_C$. The diffusion of the test particle evolving according to the Langevin dynamics can be calculated if the velocity autocorrelation function is known [8]. This yields for our system

$$\langle \Delta \vec{r}^2(t) \rangle = 4Dt[1 - \exp(-t/t_C)]. \tag{5}$$

It is evident from Eq. (5) that particle motion exhibits two different asymptotic regimes. For $t \ll t_C$, the motion is ballisticlike with $\langle \Delta \vec{r}^2(t) \rangle \propto \frac{D}{t_C} t^2$, whereas for $t \gg t_C$ it is diffusive with $\langle \Delta \vec{r}^2(t) \rangle \propto Dt$. Using t_C and D as adjustable parameters, the data in Fig. 3 could be fit reasonably well using the above simple model except at very small times. The quality of the fit could also be shown by plotting $\langle \vec{r}(t)^2 \rangle / 4Dt_C$ vs t/t_C for different n. In this case a universal curve $f(x) = x(1 - e^{-x})$ should result and was indeed observed as delineated in the inset in Fig. 3. Since no clear t^2 regime was observed, our measurement thus did not rule out the possibility that α in short times could be somewhat less than 2. The above fitting procedure allowed us to extract D and t_C as a function of n. To a good approximation, both D and t_C were found to depend linearly on n as shown respectively by the circles and the squares in Fig. 4. One could also calculate the rms distance of the particles in time t_C, $\ell_C = \sqrt{\langle \Delta \vec{r}^2(t_C) \rangle}$, which is a crude measure of the size of the coherent structures in the flow. In this case, ℓ_C was also found to increase linearly with n as delineated by the triangles in Fig. 4. Since by definition $v_{\rm rms} (\equiv \langle v(0)^2 \rangle^{1/2}) = \sqrt{2D/t_C}$, one expects that $v_{\rm rms}$ of the particle is independent of n. This was found to be approximately the case, and numerically $v_{\rm rms} \simeq 5.0 \pm 1.5$ μm/s. Constancy of $v_{\rm rms}$ also implied $\ell_C \simeq v_{\rm rms} t_C$, which we checked by plotting ℓ_C vs t_C as shown in the inset in Fig. 4. A linear regression to the data gave the slope $v_{\rm rms} \simeq 6.2$ μm/s, which is consistent with the calculation using $v_{\rm rms} = \sqrt{2D/t_C}$.

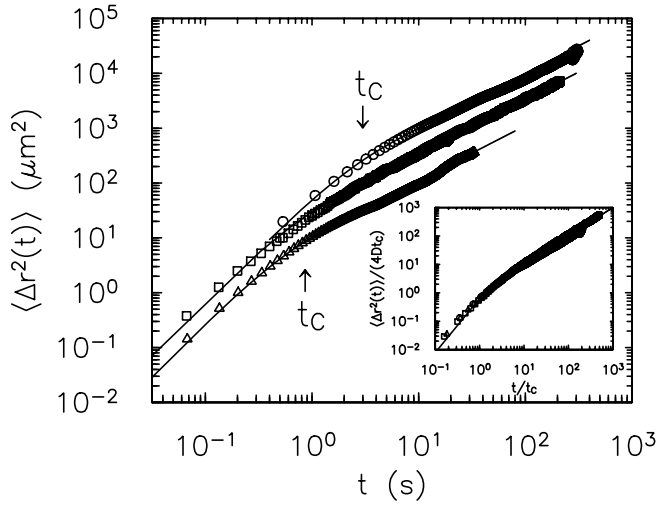

FIG. 3. The MSD of 10 μm beads at different bacterial concentrations n. The triangles, squares, and circles are, respectively, $n = 0.67$, 1.34, and 5.35×10^{10} cm^{-3}. The crossover time t_C, indicated by the arrows, increases with n. The measurements could be fit to Eq. (5) as delineated by the solid lines. The inset is the scaling plot as discussed in the text.

This experiment raises some interesting questions concerning the physics of an array of self-propelling objects and their interactions with passive particles. One of the intriguing questions is how the energy is distributed among different members of the system. Since the $v_{\rm rms}$ of the

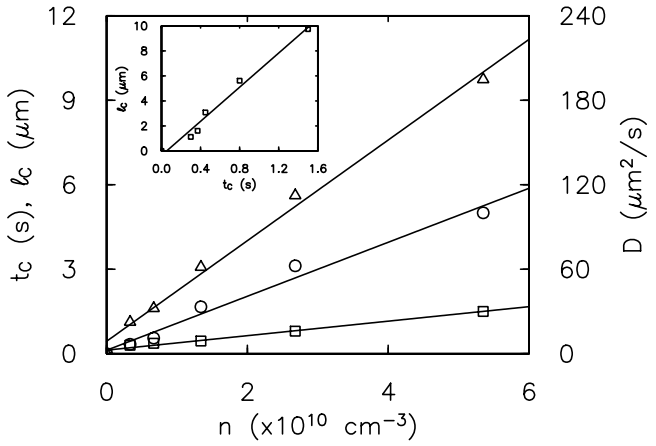

FIG. 4. The effects of bacterial concentration on t_C (squares), ℓ_C (triangles), and D (circles). The inset is ℓ_C vs t_C.

beads in the experiment was independent of n, $v_{\rm rms}$ must be a simple function of the velocity of bacteria v_0 and some geometrical factors of the bacteria and the beads. In general one may write $v_{\rm rms}^2/v_0^2 = (a/R)^\beta$, where a is some effective radius of the bacteria. This property is expected for Brownian particles in thermal equilibrium, since in this case equipartition of energy ensures that the particles and the solvent molecules share the same amount of energy k_BT. Thus the mean-square velocity ratio must be inversely proportional to the mass ratio, giving $\beta = 3$. For our experiment, since $D_{\rm eff} \sim v_{\rm rms}^2 t_C \sim 1/R$ and t_C is expected to be a property of the background fluid and the bacteria (not that of the beads), it suggests $\beta = 1$. This observation therefore indicates that the simple mechanism of equipartition of energy does not apply to our system and that hydrodynamic interactions must play a significant role.

Another intriguing issue is the spontaneous organization of bacteria to form swirls and jets that are many times their body size. Certain bacteria are known to swim up or down gradients formed by chemicals (chemotaxis), light (phototaxis), or temperature (thermotaxis). The average unidirectional motion of the bacteria when coupled to the gravitational field can cause instabilities akin to Rayleigh-Bénard convection in a layer of fluid heated from below. Such phenomena, termed bioconvection, have been studied extensively [1]. In our system, however, there was no identifiable gradient. The small film thickness $h \simeq 10\ \mu$m, which gave an effective Rayleigh number $\mathrm{Ra} = nw(\frac{\Delta\rho}{\rho})\frac{gh^3}{\nu D_0} \sim 1$, also seemed to rule out the possibility of a gravity-driven instability. Here, w and D_0 are, respectively, the volume and the diffusivity of a bacterium, $\Delta\rho$ is the mass density difference between the bacterium and the fluid, g is the gravitational constant, and ν is the kinematic viscosity of the fluid. In the above estimate $\Delta\rho/\rho \simeq 0.3$, and $D_0 = v_0^2\tau \simeq 4 \times 10^{-6}$ cm^2/s, with $\tau \simeq 1$ s being the average run time of the bacteria [4]. It is possible, however, that coherent structures formed by swimming bacteria can result from their volume exclusion and hydrodynamic correlation. Such effects have been exploited recently using computer simulations [9] and a spin model [10].

In our view, beads in a bacterial bath represent a new dynamic system with much of its statistical and hydrodynamic properties yet to be explored. It bears a number of features in common with colloidal suspensions and granular flows where collective behaviors are the hallmark of their dynamics [11,12]. In terms of hydrodynamics, the bacterial bath may also shed new light on an outstanding question concerning the nature of long-wavelength velocity fluctuations when a fluid is stirred at small scales by a random force field [13]. Based on general physical grounds Saffman predicted that the energy spectrum $E(k)$ should scale as k^{d-1}, where d is the spatial dimension of the system [14]. This result is believed to be robust [13] and works even for $\mathrm{Re} \ll 1$. However, there have been very few experiments that were able to create forcing at small enough scales to test this result. It remains an intriguing possibility that one can use genetic or nutritional means to alter the swimming patterns of the bacteria and thus yield different forcing characteristics.

We have benefited from conversations with U. Alon, S. Childress, W. I. Goldburg, H. Kellay, D. Jasnow, S. Leibler, B. Shraiman, P. Tong, and J. Zhang. We are grateful for many suggestions and technical assistance by U. Alon, S. Liu, B. Martin, and M. Rivera. The work is partially supported by the National Science Foundation under Grant No. DMR 9731701.

[1] T. J. Pedley and J. O. Kessler, Annu. Rev. Fluid Mech. **24**, 313 (1992).
[2] A. Einstein, Ann. Phys. (Leipzig) **17**, 549 (1905).
[3] P. A. Spiro, J. S. Parkinson, and H. Othmer, Proc. Natl. Acad. Sci. U.S.A. **94**, 7263 (1997).
[4] H. C. Berg and D. A. Brown, Nature (London) **239**, 500 (1972).
[5] U. Alon, L. Camarena, M. G. Surette, B. A. Arcas, Y. Liu, S. Leibler, and J. B. Stock, EMBO J. **17**, 4238 (1998).
[6] The plasmid expresses the GFP of the jellyfish *Aequorea* [see H. Morise *et al.*, Biochemistry **13**, 2656 (1997)]. The GFP gene is under control of a Luc promoter and the plasmid is ampicillin resistant.
[7] C. Cheung, Y. H. Hwang, X. L. Wu, and H. J. Choi, Phys. Rev. Lett. **76**, 2531 (1996).
[8] G. I. Taylor, Proc. London Math. Soc. Ser. 2 **20**, 196 (1921).
[9] T. Vicsek, A. Czirok, E. Ben-Jacob, I. Cohen, and O. Shochet, Phys. Rev. Lett. **75**, 1226 (1995).
[10] J. Toner and Y. Tu, Phys. Rev. Lett. **75**, 4326 (1995); Y. Tu, J. Toner, and M. Ulm, Phys. Rev. Lett. **80**, 4819 (1998).
[11] P. N. Segre, E. Herbozheimer, and P. M. Chaikin, Phys. Rev. Lett. **79**, 2574 (1997).
[12] J. B. Knight, H. M. Jaeger, and S. R. Nagel, Phys. Rev. Lett. **70**, 3728 (1993).
[13] D. Forster, D. R. Nelson, and M. J. Stephen, Phys. Rev. E **16**, 732 (1977).
[14] P. G. Saffman, J. Fluid Mech. **27**, 581 (1967).